Research Square

Preprints are preliminary reports that have not undergone peer review.
They should not be considered conclusive, used to inform clinical practice,
or referenced by the media as validated information.

Long-term environmental characterization across phenological stages for soybean adaptation

Stephany Malfatti Francisco
Federal University of Technology - Paraná (UTFPR)
Sabrina Costa Tartara
National Scientific and Technical Research Council (CONICET)
Carlos Walter Alfonso
National University of Luján
Federico Ariel Rizzo
National University of Luján
Tiago Olivoto
Federal University of Santa Catarina (UFSC)
Leonardo Domingues Figueiredo
GDM Genética do Brasil S.A
Nizio Fernando Giasson
GDM Genética do Brasil S.A
Glauco Vieira Miranda
Federal University of Technology - Paraná (UTFPR)
Giovani Benin
benin@utfpr.edu.br

Federal University of Technology - Paraná (UTFPR)

Research Article

Keywords: Genotype x environment interaction, multi-environment trials, Climate variability, yield stability

Posted Date: June 22nd, 2026

DOI: https://doi.org/10.21203/rs.3.rs-9818524/v1

License: This work is licensed under a Creative Commons Attribution 4.0 International License.
Read Full License

Additional Declarations: No competing interests reported.

Long-term environmental characterization across phenological stages for soybean adaptation

Stephany Malfatti Francisco[a], Carlos Walter Alfonso[b], Sabrina Costa Tartara[b, c], Federico Ariel Rizzo[b], Tiago Olivoto[d], Leonardo Domingues de Figueiredo[e], Nizio Fernando Giasson[e], Glauco Vieira Miranda[a], Giovani Benin[a]*

a Federal University of Technology - Paraná (UTFPR), Pato Branco, PR, Brazil
b National University of Luján, BA, Argentina
c National Scientific and Technical Research Council (CONICET), Argentina
d Federal University of Santa Catarina (UFSC), Florianópolis, SC, Brazil
e GDM Genética do Brasil S.A., Cambé, PR, Brazil

**Corresponding author:* E-mail: benin@utfpr.edu.br

Abstract

Background

Understanding how soybean cultivars (*Glycine max* (L.) Merrill) respond to climatic variability is essential for sustaining crop productivity under increasingly challenging environmental conditions. This study aimed to delineate target population environments (TPEs) and identify soybean genotypes with superior adaptability using an envirotyping framework. Grain yield data from 25 genotypes evaluated across 14 locations during the 2023/24 growing season were integrated with a 10-year historical dataset of climatic covariates. Environmental characterization was based on 11 climatic variables across five developmental stages.

Results

Four distinct TPEs were identified, capturing the main sources of environmental variability across the testing network. TPE1 was associated with moderate thermal and atmospheric conditions, favored crop establishment, whereas TPE2 exhibited greater climatic variability, particularly in temperature and atmospheric demand, indicating higher exposure to episodic stress. TPE3 showed the most stable environmental pattern, with balanced temperature and water availability, while TPE4 represented the most restrictive environment, characterized by frequent precipitation deficit and elevated vapour pressure deficit.

Conclusion

Genotypic performance varied across TPEs, revealing clear patterns of specific adaptation. Selected genotypes exhibited superior performance and stability within each TPE, highlighting the presence of both broadly and specifically adapted materials. These findings demonstrate the strategic value of environmental stratification for improving cultivar recommendation and supporting breeding decisions under climate variability.

Keywords: Genotype x environment interaction; multi-environment trials; Climate variability; yield stability

1. Introduction

Soybean (*Glycine max* (L.) Merrill) is one of the world's most economically and socially important agricultural crops. According to the Companhia Nacional de Abastecimento [1], Brazilian grain production reached approximately 177.99 million tonnes in the 2025/26 growing season, cultivated over 48.43 million hectares, with an average yield of 3.675 kg ha^{-1}, reflecting the continued expansion and high productivity of soybean cultivation in Brazil. Continued growth in global food demand, combined with the effects of climate change, has intensified the need to develop more resilient cultivars capable of maintaining high productivity under diverse environmental conditions [2, 3]. This scenario highlights the importance of a deeper understanding of the physiological and agronomic responses of genotypes to environmental fluctuations [4].

In this context, studies focused on genotype × environment interaction (GxE) have gained increasing attention because they enable the estimation of parameters describing the differential behaviour of genotypes across a range of environments and help identify materials with superior agronomic performance [5]. To achieve this, it is essential to conduct multi-environment trials (METs) across years and locations in order to identify superior genotypes on the basis of mean performance and yield stability [6, 7]. The delineation of mega-environments and the analysis of their interrelationships are fundamental tools for agronomists and plant breeders, as they allow the identification of genotypes with broad or specific adaptation [8, 9]. This approach aims primarily to reduce the effects of GxE, which arise when the performance of a given genotype varies according to environmental conditions [10, 11]. Therefore, defining breeding zones assists in identifying regions in which particular genotypes exhibit greater stability and consistent performance, thereby optimising cultivar recommendation and placement according to the predominant edaphoclimatic conditions within each mega-environment [12].

Multi-environment trials (METs) are strategically designed to sample and represent a Target Population of Environments (TPEs), defined as the set of current and prospective production environments in which candidate cultivars are expected to be deployed. Conceptually, a TPE encompasses a bounded environmental domain characterized by specific combinations of climatic, edaphic, and management-related factors that jointly determine the adaptive landscape for genotypes. Within these environmental boundaries, a subset of genotypes is expected to express superior mean performance and/or greater stability, as their genetic architecture is better aligned with the prevailing environmental drivers.

The delineation of TPEs aims to cluster locations that share similar environmental profiles, thereby maximizing the genetic correlation of genotype performance across sites within the same group) [13]. When environmental heterogeneity is structured into well-defined TPEs, the proportion of crossover genotype × environment interaction (G×E) within each group tends to decrease, and variance components attributable to non-systematic environmental noise are minimized. Consequently, the predictability of genotypic performance increases, enhancing selection accuracy and genetic gain. Within this framework, precise environmental characterization becomes a central requirement for optimizing TPEs design, refining mega-environment classification, and improving decision-making in cultivar recommendation and breeding strategies.

Recent advances in phenomics and genomics have enabled new approaches for studying the relationships between genotypes and environmental variables. Among these, envirotyping (or environmental typing) stands out because it enables the detailed characterization and analysis of environmental data for phenotypic prediction, mega-environment identification, and the grouping of similar environments [14]. Abiotic stresses act simultaneously and interactively, intensifying their negative effects on plant growth, development, and productivity [15]. In this context, envirotyping becomes a strategic tool, as it helps mitigate the influence of GxE by directing genetic improvement towards better defined target populations [16], thereby increasing the efficiency of selecting adapted genotypes. However, although envirotyping approaches have been increasingly adopted in breeding programs, studies integrating long-term climatic characterization across phenological stages to delineate soybean target population environments remain limited, particularly under subtropical production systems. Furthermore, the temporal dynamics of climatic drivers across crop development stages and their contribution to genotype adaptation patterns remain insufficiently explored. Consequently, the objective of the present study was to delineate target population environments using long-term environmental information and envirotyping techniques, as well as to identify soybean genotypes with superior adaptation and stability within the identified TPEs.

2. Materials and Methods

2.1 Evaluation of genotypes across multiple locations

Grain yield (GY) data were obtained from Value of Cultivation and Use (VCU) trials belonging to the soybean breeding programme of GDM Genética do Brasil S.A. The trials were carried out at 14 locations in southern Brazil, all within the soybean macro-region 1 (MRS 1). Figure 1 shows the geographical distribution of the testing sites and the corresponding number of environments.

Table S1, presents the altitude, latitude and longitude of each trial location. Site altitude ranged from 362 to 1,020 m. The trials were conducted during the 2023/24 growing season, and 25 genotypes were evaluated (10 cultivars and 15 breeding lines) with maturity groups ranging from 5.1 to 5.6 (Table S2).

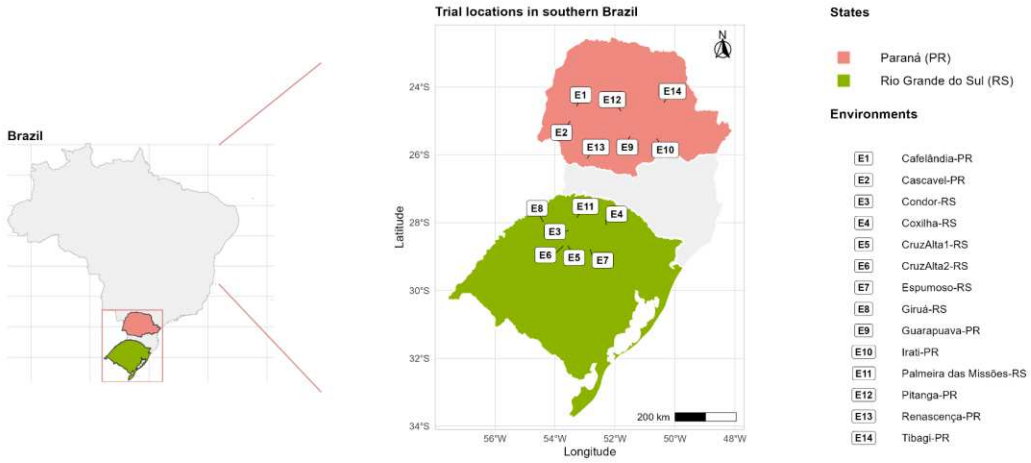


Fig. 1. Geographic distribution of the experimental environments used for the competitive evaluation of soybean genotypes during the 2023/24 growing season in southern Brazil. The inset map highlights the location of Paraná and Rio Grande do Sul within Brazil, whereas the enlarged map shows the spatial distribution of the 14 trial sites identified as environments (E1–E14).

The experiment followed a randomised complete block design with three replications. Experimental units consisted of plots with four rows, each 5 m long and spaced 0.5 m apart, resulting in a harvested area of 10.0 m². Grain yield of the cultivars and breeding lines was calculated from the yield obtained in the harvested area of each plot (kg plot^{-1}), adjusted to 13% moisture, and subsequently expressed in kg ha^{-1}. Crop management practices followed the technical recommendations for soybean at each location.

To define the Target Population of Environments (TPEs), meteorological data were obtained using the get_weather() function from the R package EnvRtype [8]. Climatic information was retrieved from NASA's Prediction Of Worldwide Energy Resources (NASA POWER) database, which provides global meteorological data derived from satellite observations and climate models. A 10-year historical climatic dataset (2013–2023) was used to represent the prevailing environmental conditions of each trial location. Meteorological variables were extracted using the geographical coordinates of each experimental site together with the respective sowing and harvest dates, ensuring that the climatic covariates corresponded to the soybean crop cycle. Initially, 30 environmental covariates were obtained. After quality-control procedures, variables showing high multicollinearity were removed. Subsequently, covariates considered more relevant to soybean development were retained, resulting in a final set of 11 environmental covariates used in the analyses (Table 1).

Table 1 Climatic covariates obtained from the NASA POWER database and derived environmental variables used for the characterization of trial environments

Source	Covariate	Description	Unit
NASA POWER	PAR	Photosynthetically active radiation	μmol m^{-2} s^{-1}
	RHU	Relative humidity	%
	T2M	Mean air temperature	°C day^{-1}
	TMX	Maximum temperature	°C day^{-1}

	TMN	Minimum temperature	°C day^{-1}
Calculated	ETP	Evapotranspiration	mm day^{-1}
	PRT	Total precipitation	mm day^{-1}
	SDU	Actual sunshine duration	h
	PHO	Maximum photoperiod	h
	PRD	Precipitation deficit	mm day^{-1}
	VPD	Vapor pressure deficit	kPa

The W_matrix() function from the same package was used to create a matrix of climatic covariates (W), as proposed by [8].

The environmental kernel matrix was computed using the following expression:

$$K_E = \frac{CC'}{(tr(CC')/n)} + I\varepsilon \quad (1)$$

Where K_E represents the environmental similarity matrix, C' is the matrix of standardized environmental covariates, composed of standardized climatic covariates (e.g., temperature, radiation, precipitation, and atmospheric variables), across environments. The term CC' corresponds to the cross-product of the environmental covariates matrix, capturing the pairwise similarity between environments based on their multivariate profiles. The expression $tr(CC')/n$, where $tr(\cdot)$ denotes the trace of the matrix and n is the number of environments, is used as a scaling factor to normalize the kernel and ensure comparability across datasets. The term $I\varepsilon$ was included to ensure numerical stability.

To identify the Target Population of Environments (TPEs), the environmental kernel matrix was subjected to hierarchical clustering using the average-linkage method. This approach enabled the visualization and grouping of environments based on their climatic similarity, supporting the interpretation of genotype performance across contrasting environmental conditions. The kernel matrix quantifies the environmental proximity between pairs of environments on the basis of the multivariate set of climatic covariates. Thus, environments with similar covariate profiles exhibit greater similarity, enabling: (i) the modeling of GxE interactions through reaction-norm approaches; (ii) the stratification of macro-environments (TPEs); and (iii) the incorporation of environmental relationships into prediction models, in a manner analogous to the genomic relationship matrix (GRM) used for genotypes [17].

To capture temporal variation throughout the crop cycle, the env_typing() function from the EnvRtype package was used to generate environmental typologies according to the selected covariates. These were divided into five developmental stages: 1-VE (emergence); 2-VE/R2 (vegetative stage); 3-R3/R5 (pod development); 4-R5/R6 (grain filling); and 5-R7/R8 (physiological maturity). Frequency distributions were computed using the quantiles 0.00, 0.25, 0.50, 0.75, and 1.00.

Phenotypic data were initially inspected for potential violations of statistical assumptions. Residual normality was evaluated using the Shapiro–Wilk test, and homogeneity of variances was assessed using Bartlett's test. Data processing and exploratory analyses were performed using the metan package [18] together with functions from the tidyverse ecosystem

[19]. Potential outliers were evaluated using residual diagnostics; no observations met the predefined exclusion criterion, and therefore all observations were retained in the final analyses. G×E interaction, was analysed using a linear mixed model, with genotypes and environments as random effects.

The data were analysed using the following linear mixed model:

$$Y_{ijk} = \mu + G_i + E_j + (GE)_{ij} + Bk_i + \varepsilon_{ijk} \quad (2)$$

where Y_{ijk} represents the observed grain yield of genotype i in environment j and replication k; μ is the overall mean; G_i is the random effect of genotype i; E_j is the random effect of environment j; $(GE)_{ij}$ represents the genotype × environment interaction; Bk_i is the random effect of block k nested within environment j; and ε_{ijk} is the residual error. Variance components were estimated using the restricted maximum likelihood (REML) method, and the best linear unbiased predictions (BLUPs) were obtained for genotypic effects.

To explore the structure of the G×E interaction, the matrix of BLUPs associated with the interaction effects was subjected to singular value decomposition, generating a BLUP-based biplot. The first two principal components were used to graphically represent the relationship between genotypes and environments, allowing the identification of differential responses and patterns of adaptability across environments.

Genotype adaptability and stability were evaluated using the WAASB (Weighted Average of Absolute Scores) index proposed by [18]. This approach combines the decomposition of the genotype × environment interaction through singular value decomposition with mixed-model predictions, allowing simultaneous evaluation of mean performance and stability.

The WAASB index is calculated as:

$$WAASB_i = \frac{\sum_{k=1}^{p} |IPCA_{ik}| \, EP_k}{\sum_{k=1}^{p} EP_k} \quad (3)$$

where $IPCA_{ik}$ is the score of genotype i in the k -th interaction principal component axis and EP_k represents the variance explained by that component.

Lower WAASB values indicate greater stability across environments. The relationship between mean grain yield (BLUPs) and WAASB values was used to classify genotypes according to their productivity and stability, allowing the identification of genotypes combining high performance and wide adaptability.

Prior to analysis, environmental covariates were standardized to remove scale effects. Principal component analysis (PCA) was then performed to summarize the main sources of environmental variation and to identify climatic gradients among environments. Results were visualized using a PCA biplot, which allowed the joint representation of climatic variables and the target population of environments (TPEs), thereby facilitating the identification of environmental drivers associated with the observed variability across the testing network.

All statistical analyses were performed using R software [19]. The authors declare that generative artificial intelligence (AI) tools were used exclusively to assist in R programming

and code development. All data processing, statistical analyses, interpretation of results, and scientific conclusions were performed exclusively by the authors. Generative AI was not used for scientific decision-making, data interpretation, or drawing research conclusions.

3. Results and Discussion

3.1 Variance components and genotype × environment interaction

The analysis of variance revealed highly significant differences ($p < 0.01$) for the effects of environments, genotypes, and genotype × environment interaction on GY, indicating variability in genotypic responses and the presence of contrasting environments. The block effect was not significant, showing that variation among blocks was small. The overall coefficient of variation was 5.84%, which is considered low and indicates high experimental precision (Table S3). Across environments, coefficients of variation ranged from 3.00% to 8.75%, also indicating good experimental precision. According to [20], such values are considered typical for agricultural field trials (Table S4). Mean grain yield ranged from 3341.19 kg ha^{-1} in environment E8 to 5561.71 kg ha^{-1} in environment E10. Broad-sense heritability (H^2) was high in most environments, ranging from 0.40 in Cruz Alta1-RS (E5) to 0.97 in Palmeira das Missões-RS (E11). Heritability represents the proportion of phenotypic variance explained by genetic variance within a population, indicates the potential response to selection [21]. Values range from 0 to 1, with values closer to 1 indicating a greater genetic influence on the phenotype, whereas values closer to 0 indicate stronger environmental influence and greater variability [22, 23].

Most environments evaluated exhibited favourable H^2 estimates, indicating high reliability for genotype selection. Palmeira das Missões-RS (E11), Espumoso-RS (E7), Condor-RS (E3), Pitanga-PR (E12), and Cascavel-PR (E2) stood out with heritability values above 0.90, demonstrating low environmental influence on trait expression and a greater contribution from the genetic component. These results reinforce the potential of these environments for more precise and efficient genotype discrimination. Conversely, Cruz Alta1-RS (E5) exhibited the lowest H^2 (0.40), indicating strong environmental influence on the trait and, consequently, lower confidence for selection in this environment. Overall, most environments presented H^2 values above 0.80, favouring the identification of superior genotypes.

The analysis of GxE interaction based on BLUPs obtained from the linear mixed model revealed a clear pattern of differential response among genotypes across environments, summarized by the first two principal components of the interaction matrix. PC1 explained 26.3% and PC2 explained 17.1% of the total G×E variation, jointly accounting for 43.4% of the variation represented in the biplot. In multi-environment trials, decomposition of the predicted interaction matrix provides an effective approach to identify both genotypes with specific adaptation and environments with greater discriminating ability [18, 24]. When based on BLUPs, this strategy allows a more appropriate modelling of random effects and improves inference regarding genotype adaptability and stability.

In the biplot representation, points located farther from the origin indicate a greater contribution to the G×E interaction, whereas points close to the origin indicate lower interaction effects and more stable behavior. According to this criterion, environments Irati-PR

(E10), Renascença-PR (E13), Girua-RS (E8), Cruz Alta1-RS (E5), and Coxilha-RS (E4) were the most influential environments in the interaction structure (Figure 2).

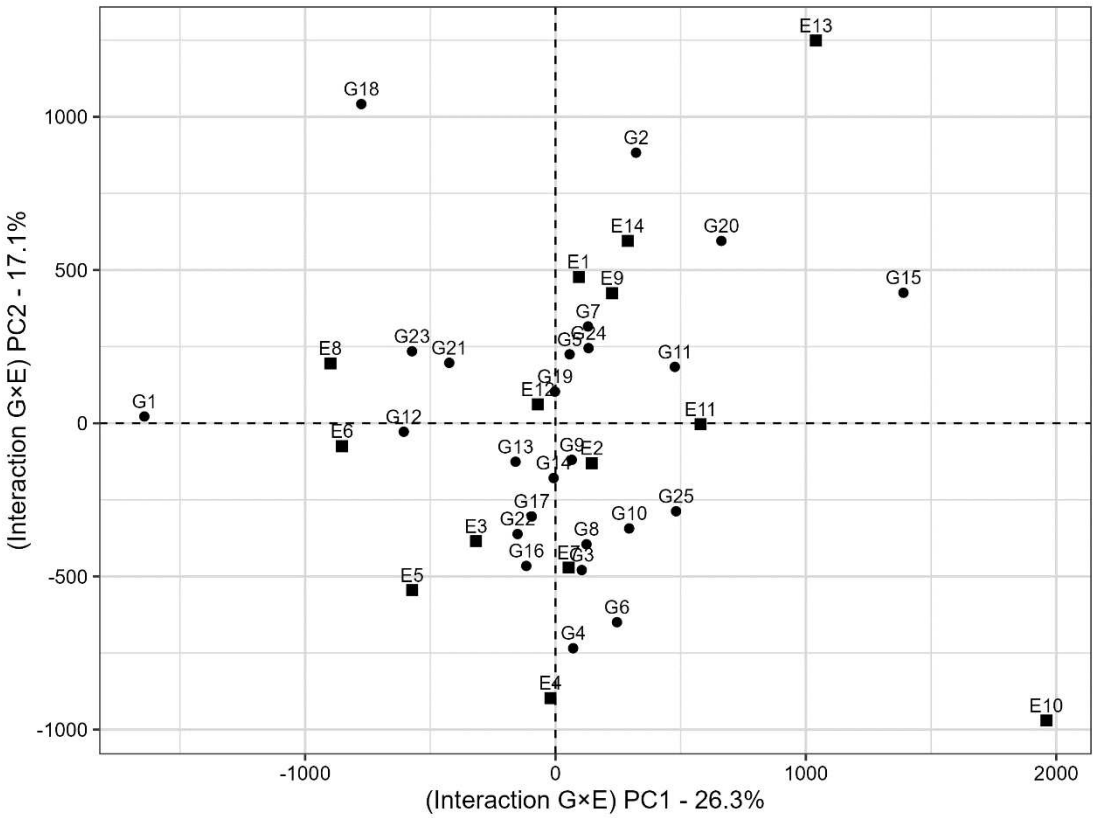


Fig. 2. Biplot of the genotype × environment interaction (G×E) based on BLUPs for grain yield, showing the relationship between genotypes and environments across the first two principal components.

Irati-PR (E10) showed the greatest distance from the origin, with a strong positive association with PC1 and a negative association with PC2, indicating a highly contrasting environmental pattern relative to the other testing sites. Renascença-PR (E13), also exhibited strong discriminating ability, with high positive scores on both axes, whereas Giruá-RS (E8) was positioned in the opposite direction of PC1, suggesting a distinct environmental profile. CruzAlta1-RS (E5) and Coxilha-RS (E4), both with negative scores on PC2, contributed to differentiating genotypes sensitive to less favorable conditions or showing specific responses along this interaction gradient. In contrast, environments such as Palmeira das Missões-RS (E11), Pitanga-PR (E12), Cascavel-PR (E2), and, to a lesser extent, Espumoso-RS (E7) were located closer to the origin, indicating a smaller contribution to G×E and a behavior more representative of the overall environmental mean. These patterns are consistent with previous studies, in which environments positioned farther from the origin tend to be more informative for genotype discrimination [25, 26].

Among the evaluated genotypes, LI4E (G15), LI7H (G18), 511 IPRO (G2), LI9J (G20), 50I52RSF IPRO (G1), 531 I2X (G6), and C2531 E (G4) showed the strongest association with the G×E interaction, as indicated by their greater distance from the origin. Genotype LI4E (G15) presented high positive scores on both PC1 and PC2, suggesting a strong response to

specific environmental conditions represented by environments located in the upper-right quadrant of the biplot, particularly those associated with Renascença-PR (E13). This pattern indicates specific adaptation rather than broad stability. Genotype LI7H (G18) exhibited negative PC1 scores and high positive PC2 values, indicating a contrasting interaction pattern and adaptation to a different set of environmental conditions. Genotypes 511 IPRO (G2) and LI9J (G20) also showed strong positive associations with PC1, whereas 531 I2X (G6) and C2531 E (G4) were characterized by negative PC2 values, suggesting greater responsiveness to environments positioned in the lower region of the biplot. Genotype 50I52RSF IPRO (G1) presented a large displacement in the negative direction of PC1, indicating a distinct interaction pattern compared with most other genotypes. In contrast, genotypes such as LI8I (G19), LI13N (G24), LI3D (G14), LI1B (G12), and LI2C (G13) were located closer to the origin, indicating a smaller contribution to the G×E interaction and a more predictable performance across environments. In multienvironment trials, genotypes positioned near the origin are generally considered more stable because they interact less with environmental variation [27].

Overall, environments Irati-PR (E10) and Renascença-PR (E13) were the most contrasting environments and potentially the most informative for genotype discrimination, whereas genotypes LI4E (G15), LI7H (G18), 511 IPRO (G2), and LI9J (G20) exhibited the strongest specific responses. Conversely, genotypes located closer to the origin, such as LI8I (G19), LI13N (G24), and LI10K (G21), tended to show more balanced performance across environments. These results demonstrate that the G×E biplot derived from the mixed model effectively captured the interaction structure, allowing the identification of specifically adapted genotypes and key environments for environmental stratification and future recommendation strategies.

The distribution of genotypes and environments across opposite quadrants also suggests the presence of crossover interaction, indicating changes in genotype ranking across environments. This type of interaction is particularly relevant for breeding programs targeting both broad and specific adaptation. Genotypes located near particular environments in the biplot may present superior relative performance under similar environmental conditions [28, 29], whereas genotypes positioned closer to the origin may be preferable when the goal is greater performance predictability. Mixed linear models combined with BLUP-based biplots have increasingly been recommended because they integrate statistical robustness, improved handling of unbalanced data, and intuitive graphical interpretation of G×E patterns [30, 31, 18]. Environmental similarity among testing locations is essential for understanding genotype × environment interaction (G×E) and defining the target population of environments (TPE) in multi-environment trials. In this study, climatic similarity among environments was assessed using 10 years of meteorological data obtained from the NASA POWER database, allowing the characterization of long-term environmental patterns and reducing the influence of short-term climatic variability (Figure 3).

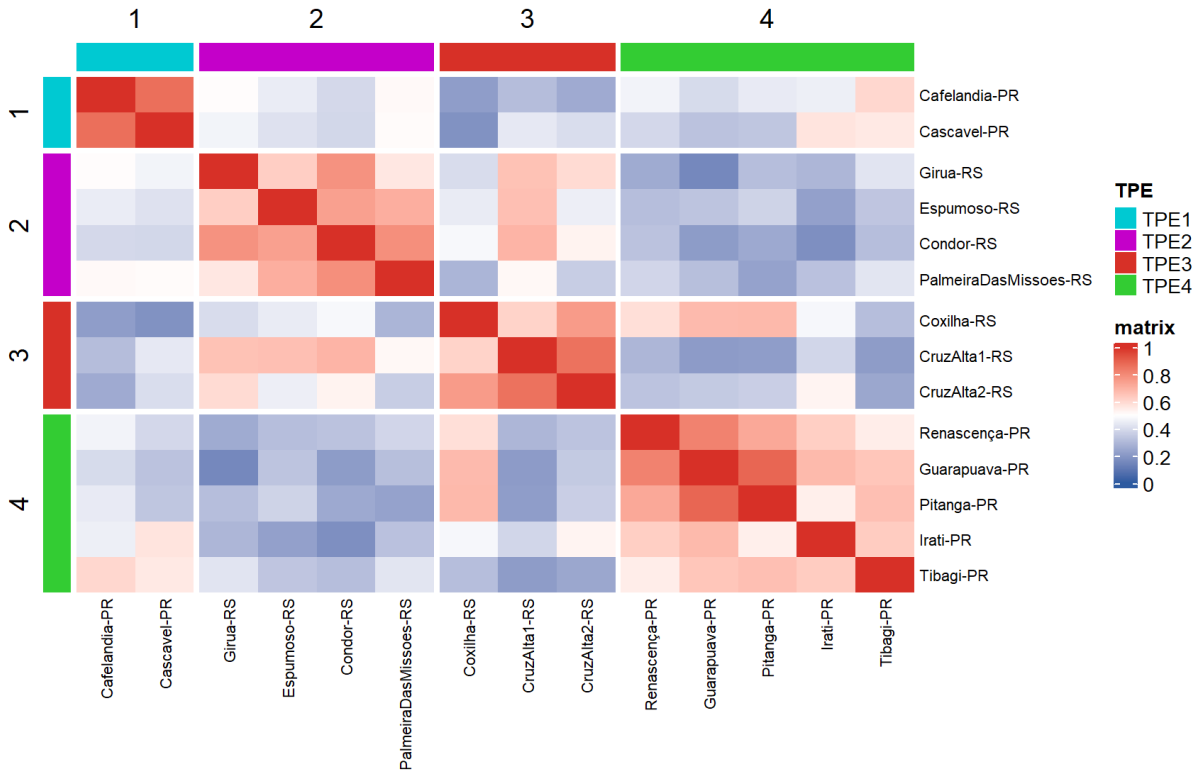


Fig. 3. Heatmap showing the TPE identified based on similarity among environments using a 10-year historical dataset of environmental covariates obtained from the NASA POWER database: T2M (mean temperature), TMX (maximum temperature), TMN (minimum temperature), PAR (photosynthetically active radiation), PRT (total precipitation), PRD (precipitation deficit), RHU (relative humidity), VPD (vapor pressure deficit), SDU (sunshine duration), PHO (photoperiod), and ETP (potential evapotranspiration).

The similarity matrix was summarized through hierarchical clustering, and the resulting heatmap revealed four distinct environmental clusters, defined as TPE1–TPE4. TPE1 included sites located in the state of Paraná, generally characterized by mid to high-altitude conditions (600–720 m), moderate temperature regimes, and adequate soil moisture during the growing season. TPE2 comprised sites in the northwestern region of Rio Grande do Sul, featuring intermediate altitudes (420–630 m) and a humid subtropical climate (Cfa) with hot summers and well-distributed rainfall throughout the year. This region is one of the main soybean-producing areas of the state and has strong agricultural relevance. TPE3, also located in Rio Grande do Sul, exhibited medium altitudes (370–715 m) and was geographically close to TPE2.

However, TPE3 differed from TPE2 in rainfall patterns and thermal amplitude. This distinction highlights the environmental heterogeneity that can exist even within the same geographical region. Finally, TPE4, located in Paraná, is characterized by higher altitudes (790–1020 m), and cooler temperatures throughout the crop cycle. These conditions may limit the performance of genotypes that require higher temperatures [32].

The PCA biplot enabled the joint representation of climatic covariates and environmental clusters, allowing the visualization of the associations among the Target Population of Environments (TPE) and the environmental variables explaining their variability. To better understand the environmental drivers underlying the stratification, a PCA-based

characterization was performed using climatic covariates derived from NASA POWER data. The first two principal components explained 73.6% of the total environmental variation, with Dim1 accounting for 57.1% and Dim2 for 16.5%.

TPE1 (Cafelândia-PR (E1); Cascavel-PR (E2)), positioned in the upper-right quadrant, showed strong association with minimum temperature (TMN), mean temperature (T2M), maximum temperature (TMX), photosynthetically active radiation (PAR), and precipitation deficit (PRD). This environmental profile suggests warmer growing conditions combined with elevated radiation availability and moderate atmospheric demand. Higher thermal load throughout crop development may accelerate phenological progression, shorten reproductive periods, and alter carbon allocation dynamics, potentially affecting assimilate partitioning during pod formation and grain filling. In addition, increased radiation availability may enhance photosynthetic activity under favorable water conditions but can intensify atmospheric demand when combined with elevated temperatures. These conditions may favour genotypes with improved stomatal regulation, greater transpiration efficiency, and enhanced tolerance to transient water limitation, ultimately shaping genotype-specific adaptation patterns (Figure 4).

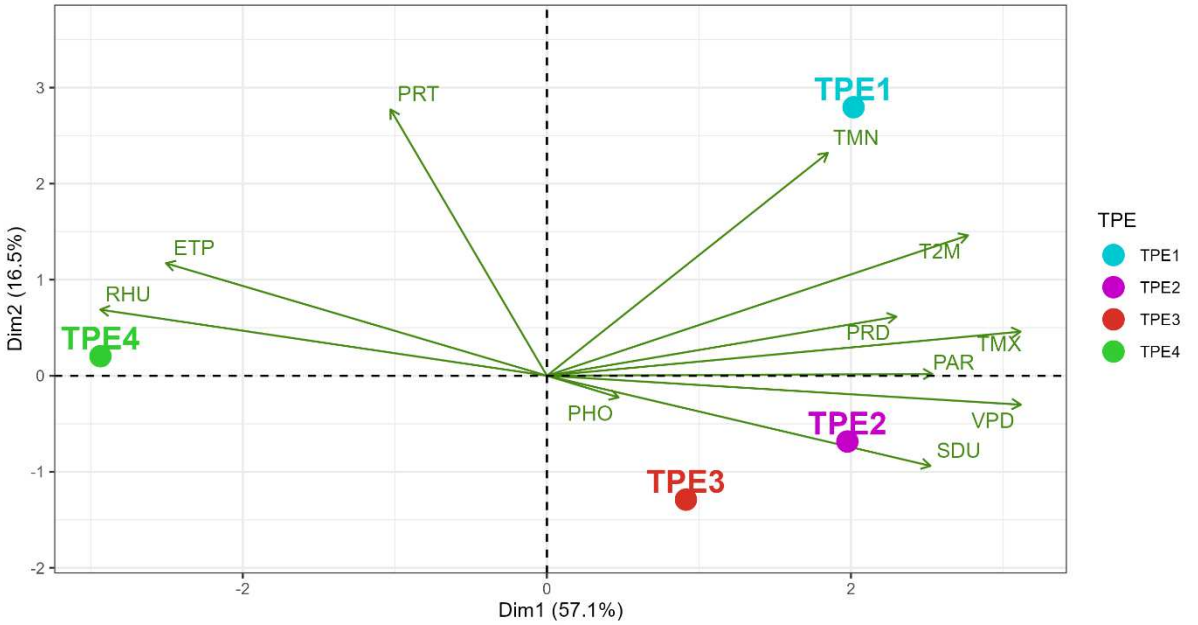


Fig. 4. PCA biplot illustrating the relationships among climatic covariates and the environmental clusters (TPE1–TPE4). The analysis was based on crop-cycle aggregated climatic data from the 2023/24 growing season. The variables included were T2M (mean temperature), TMX (maximum temperature), TMN (minimum temperature), PAR (photosynthetically active radiation), PRT (total precipitation), PRD (precipitation deficit), RHU (relative humidity), VPD (vapor pressure deficit), SDU (sunshine duration), PHO (photoperiod), and ETP (potential evapotranspiration).

TPE2 (Condor-RS (E3); Espumoso-RS (E7); Giruá-RS (E8); Palmeira das Missões-RS (E11)), located in the lower-right quadrant, was primarily associated with vapor pressure deficit (VPD) and sunshine duration (SDU), indicating environments characterized by greater evaporative demand and increased atmospheric dryness. Elevated VPD directly influences plant water relations by increasing transpiration rates and promoting stomatal closure, which may reduce carbon assimilation efficiency and biomass accumulation even under adequate soil

water availability. Increased atmospheric demand during reproductive stages may intensify physiological drought responses and compromise reproductive stability, particularly during flowering and grain filling. Under these conditions, genotypes capable of maintaining physiological homeostasis through efficient stomatal control and water-use efficiency may exhibit superior adaptation and productivity.

TPE3 (Coxilha-RS (E4); Cruz Alta1-RS (E5); Cruz Alta2-RS (E6)), also positioned on the right side of the biplot, showed stronger association with sunshine duration (SDU) and photoperiod (PHO), with secondary contribution from vapor pressure deficit (VPD). This environmental configuration indicates conditions with greater radiation exposure and longer periods of solar availability combined with moderate atmospheric demand. Photoperiod and radiation availability influence soybean developmental timing, canopy expansion, and biomass accumulation, directly affecting source–sink relationships throughout crop development. Compared with the other TPEs, this group exhibited greater climatic stability, potentially reducing environmental fluctuations affecting reproductive development and grain formation. Such conditions may favour genotypes with stable physiological performance and greater capacity to maintain assimilate production under relatively predictable environmental conditions.

TPE4 (Guarapuava-PR (E9); Irati-PR (E10); Pitanga-PR (E12); Renascença-PR (E13); Tibagi-PR (E14)), positioned on the left side of the biplot, was strongly associated with relative humidity (RHU), precipitation (PRT), and evapotranspiration (ETP), representing environments characterized by distinct water availability dynamics and cooler thermal regimes associated with higher altitudes. Although increased precipitation and humidity may alleviate atmospheric drought stress, greater evaporative demand combined with precipitation deficits observed during specific crop stages may impose physiological limitations affecting reproductive performance. Variations in soil water availability directly influence stomatal conductance, leaf expansion, photosynthetic efficiency, and assimilate translocation to developing seeds. The combination of cooler temperatures and fluctuations in water availability may favour genotypes exhibiting greater physiological resilience and improved capacity to maintain reproductive stability under restrictive environmental conditions.

Overall, the environmental stratification revealed distinct climatic drivers influencing soybean adaptation across southern Brazil. Thermal regime, atmospheric demand, radiation availability, and water dynamics jointly shape physiological processes associated with crop development, reproductive success, and grain formation [8, 10]. These findings reinforce that soybean adaptation results from the integrated response of genotypes to multiple environmental constraints operating simultaneously throughout crop development [33], highlighting the importance of envirotyping approaches for understanding genotype × environment interaction and improving climate-resilient breeding strategies.

The Weighted Average of Absolute Scores (WAASB) summarizes the contribution of the interaction principal components derived from the AMMI decomposition of the genotype × environment interaction, enabling the simultaneous evaluation of productivity and phenotypic stability across environments [18]. Lower WAASB values indicated greater stability, reflecting a reduced contribution of G×E interaction to genotype performance and, consequently, greater predictability across contrasting environmental conditions.

The WAASB analysis revealed substantial differences among soybean genotypes regarding adaptation patterns and environmental responsiveness (Figure 5). Genotypes positioned in the upper-right quadrant combined superior grain yield with lower WAASB values, indicating both broad adaptation and stable performance across environmental conditions. This pattern suggests greater physiological robustness and the capacity to maintain reproductive performance under contrasting climatic scenarios, an important attribute for breeding programs targeting climate resilience.

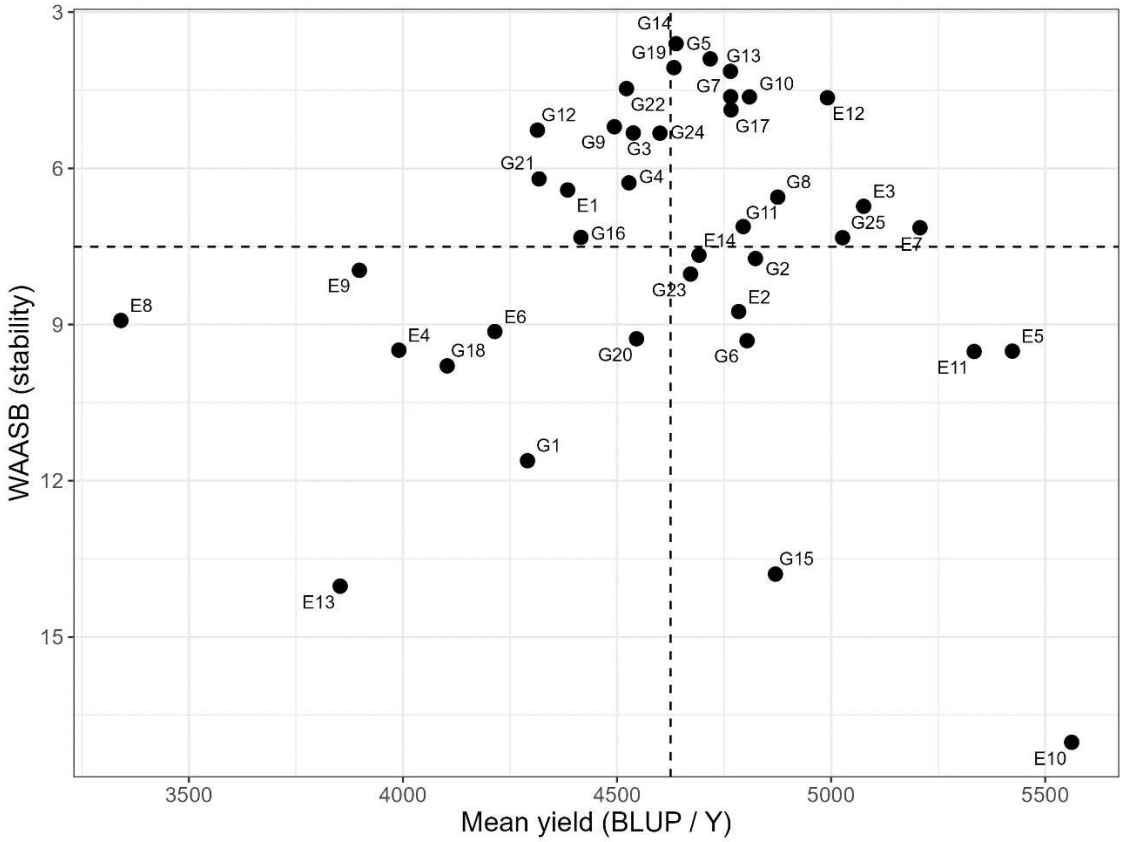


Fig. 5. WAASB (Weighted Average of Absolute Scores) versus mean grain yield (BLUPs) for genotypes and environments evaluated in multi-environment trials. The horizontal axis represents the mean yield predicted by BLUPs, while the vertical axis represents the WAASB stability index, where lower values indicate greater stability. Dashed lines indicate the overall mean values for yield and WAASB, dividing the plot into four quadrants to facilitate the identification of genotypes combining high productivity and stability across environments.

Conversely, genotypes located in the lower-right quadrant exhibited elevated productivity but greater contribution to GxE interaction, indicating stronger environmental sensitivity and potential specific adaptation. Genotype LI4E (G15), for example, combined high grain yield with lower stability, suggesting performance strongly dependent on environmental conditions. Such behaviour may reflect greater responsiveness to favourable environments but reduced performance predictability across heterogeneous production systems.

Genotypes positioned closer to the origin, including LI8I (G19), LI13N (G24), and LI10K (G21), exhibited lower contribution to G×E interaction and more balanced responses

across environmental conditions. Greater stability may indicate an enhanced capacity to maintain physiological homeostasis under environmental variability, contributing to more predictable yield expression across contrasting production environments.

Environmental effects also differed substantially. Irati-PR (E10) and Renascença-PR (E13) exhibited the highest WAASB values, indicating stronger environmental contribution to G×E interaction and greater capacity for genotype discrimination. These environments likely impose stronger climatic constraints affecting crop physiological performance, thereby increasing the expression of differential genotypic responses. In contrast, Cafelândia-PR (E1) and Tibagi-PR (E14) showed smaller interaction effects and behaved as more representative testing environments, contributing to greater predictability of genotype performance.

Overall, the WAASB approach demonstrated that soybean adaptation depends not only on yield potential but also on the capacity of genotypes to maintain stable performance under environmental variability. Integrating productivity and stability metrics provides a robust framework for identifying soybean materials combining superior agronomic performance and resilience to contrasting environmental conditions, supporting breeding strategies focused on climate adaptation.

3.2 Envirotyping

The distribution of mean air temperature (T2M) revealed clear contrasts among the four target populations of environments across soybean phenological stages (Figure 6). At the VE stage, TPE3 and TPE4 showed a higher frequency of lower temperature ranges (15.8-21.7°C and 21.7-23.6°C), whereas TPE1 was characterized by a greater frequency of higher temperature ranges (23.6–25.4 °C and 25.4–28.9 °C). From VE–R2 to R3–R5, the temperature distribution became more homogeneous among TPEs, although TPE1 still showed a greater frequency of the highest temperature ranges. During the reproductive stages (R5–R6 and R7–R8), TPE1 exhibited the highest frequency of elevated temperatures, followed by TPE2, whereas TPE3 and TPE4 remained predominantly associated with moderate temperature ranges. Overall, TPE1 was consistently associated with warmer thermal profiles throughout the crop cycle, while TPE3 and TPE4 showed more stable and less extreme temperature conditions, which may favour greater grain yield stability.

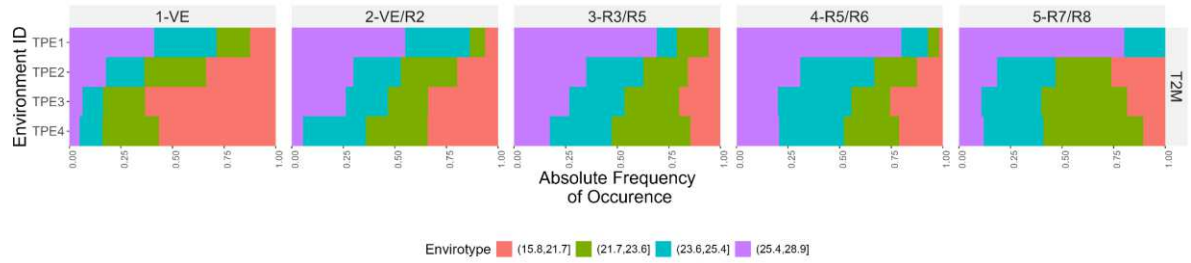


Fig. 6. Frequency distribution of mean air temperature (T2M, °C) across soybean phenological stages (VE, VE–R2, R3–R5, R5–R6 and R7–R8) in four target population environments (TPEs).

The observed thermal patterns indicate distinct physiological environments across TPEs. The predominance of warmer conditions in TPE1, particularly during reproductive

stages, may accelerate phenological progression and shorten the duration of seed filling, potentially limiting assimilate accumulation. Conversely, the more moderate thermal conditions observed in TPE3 and TPE4 may favour sustained photosynthetic activity and reproductive stability, contributing to more predictable genotype performance. Environments with moderate mean temperatures tend to sustain canopy expansion and radiation interception without accelerating phenological development [34]. Recent studies indicate that even small increases in growing-season temperature can lead to significant yield reductions, primarily due to decreased pod set and seed size [35].

The distribution of maximum air temperature (TMX) envirotypes revealed clear contrasts among TPEs throughout the soybean crop cycle (Figure 7). At the VE stage, TPE3 and TPE4 showed a higher frequency of lower temperature stages (21.2–26.7°C and 26.7–28.8°C), whereas TPE1 was characterized by a greater frequency of higher temperature ranges (28.8–30.8 °C and 30.8–35.8 °C). TPE2 exhibited a more balanced distribution across the temperature gradient. From VE-RS to R3-R5, the temperature distribution became more homogeneous among TPEs, however, TPE1 consistently maintained a higher frequency of elevated maximum temperatures compared with the other TPEs. During the reproductive stages (R5–R6 and R7–R8), TPE1 showed the highest frequency of elevated temperatures, while TPE2, TPE3 and TPE4 remained predominantly associated with lower to moderate temperature ranges. These results indicate that TPE1 is consistently exposed to greater thermal pressure throughout crop development. Elevated maximum temperatures during reproductive stages may impair pollen viability, increase flower and pod abortion, and reduce assimilate allocation to developing seeds. In contrast, the more moderate thermal conditions observed in TPE2, TPE3 and TPE4 may contribute to improved reproductive stability.

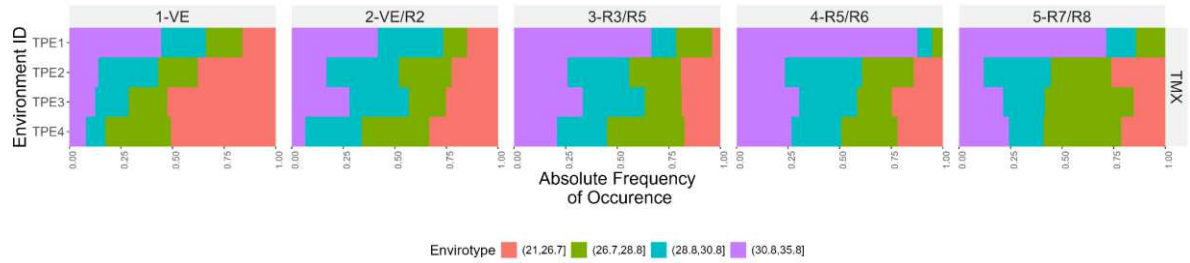


Fig. 7. Frequency distribution of maximum temperature (TMX, °C) across soybean phenological stages (VE, VE–R2, R3–R5, R5–R6 and R7–R8) in the four target populations of environments (TPEs).

Higher maximum temperatures during reproductive stages, especially in TPE1, may intensify heat stress and negatively affect reproductive processes such as pollen viability and grain filling, [36], increased flower and pod abortion and reduced seed number [37]. In contrast maximum temperatures above 30 °C are known to negatively affect pollen viability and pod formation, especially near flowering and early pod development [38]. Previous studies indicate that environments with moderate and stable temperatures favour higher radiation-use efficiency and grain accumulation [39].

Clear contrasts in relative humidity (RHU) were observed among TPEs across the soybean crop cycle (Figure 8). At the VE stage, TPE1 showed a higher frequency of lower

humidity ranges (58.5-76.1%), whereas TPE3 and TPE4 were more frequently associated with higher humidity ranges (80.9-86.2% and 86.2-94.2%). TPE2 presented a more even distribution across the humidity gradient. During VE–R2 to R3–R5, the distribution of RHU became more homogeneous among TPEs, although TPE1 still maintained a greater frequency of lower humidity, while TPE2, TPE3 and TPE4 were more frequently associated with higher humidity levels. In the reproductive stages (R5-R6 and R5–R8), TPE1 consistently exhibited lowest humidity levels, whereas TPE2, TPE3 and TPE4 remained associated with higher humidity ranges. These results indicate that TPE1 is characterized by drier atmospheric conditions throughout crop development, particularly during reproductive stages. Reduced atmospheric humidity may intensify evaporative demand and increase stomatal limitation, potentially restricting carbon assimilation under high atmospheric demand. In contrast, the more humid conditions observed in TPE2, TPE3 and TPE4 may favour improved plant water status and greater physiological stability.

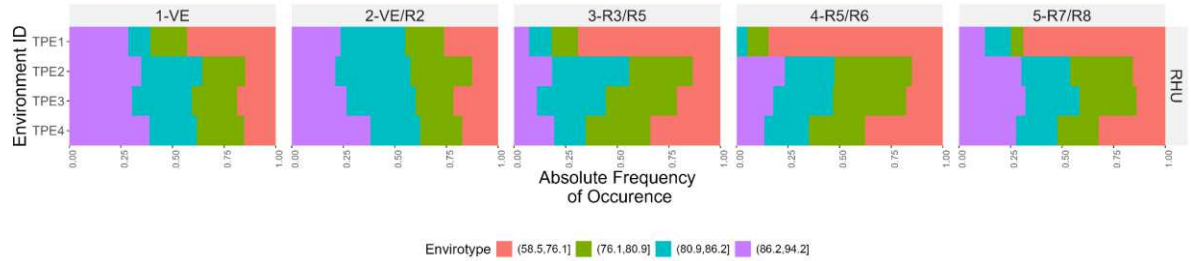


Fig. 8. Frequency distribution of relative humidity (RHU, %) across soybean phenological stages (VE, VE–R2, R3–R5, R5–R6 and R7–R8) in the four target populations of environments (TPEs).

Relative humidity influences plant water status and transpiration dynamics. Lower humidity conditions, as observed in TPE1, may increase vapor pressure deficit and intensify plant water loss, potentially reducing stomatal conductance and photosynthesis [40, 41]. During first vegetative stages, the crop shows relatively low sensitivity to water deficit, with limited impact on final yield. However, as the crop enters reproductive development, particularly from flowering to grain filling, water demand increases substantially, and the effects of low relative humidity and high atmospheric demand become more pronounced [42]. In contrast, environments with moderate humidity conditions tend to support improved plant water status, sustained carbon assimilation, and greater yield stability.

ETP showed consistent differences among TPEs throughout the crop cycle (Figure 9). At the VE stage, all TPEs exhibited a higher ETP value, indicating elevated atmospheric demand during early development. Between VE–R2 and R3–R5, intermediate ETP values became more frequent across all TPEs, reflecting a more homogeneous pattern among environments. In the R5–R8 stages, TPE2 and TPE4 showed a greater contribution of higher ETP values, indicating differences in evaporative demand during the final stages of the crop cycle.

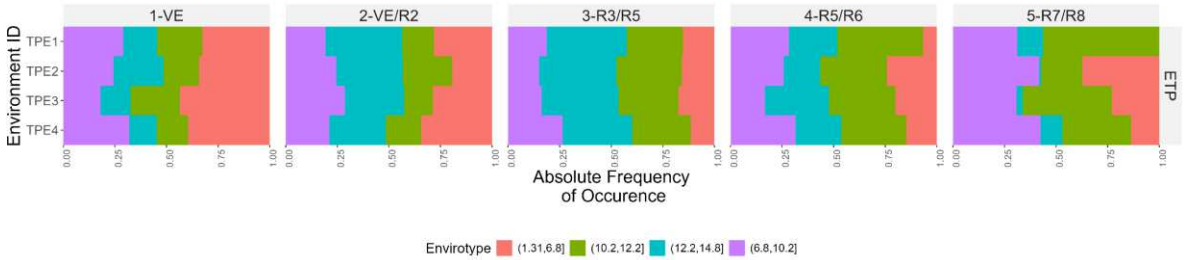


Fig. 9. Frequency distribution of evapotranspiration (ETP, mm day^{-1}) across soybean phenological stages (VE, VE–R2, R3–R5, R5–R6 and R7–R8) in the four target populations of environments (TPEs).

Evapotranspiration reflects the atmospheric demand for water and is closely related to crop water use. Elevated evapotranspiration reflects greater atmospheric demand for water and may accelerate soil moisture depletion when precipitation supply becomes limiting. The greater contribution of elevated ETP values observed in TPE2 and TPE4 during later developmental stages suggests increased atmospheric demand during grain filling, a period highly sensitive to water limitation [38]. In contrast, environments with moderate ETP, such as TPE3 and TPE4, tend to impose less atmospheric stress, contributing to improved water-use efficiency and yield stability. Water limitation, largely driven by atmospheric demand and evapotranspiration, is one of the main factors explaining yield gaps in soybean production systems [43, 44].

The distribution of precipitation envirotypes showed clear differences among TPEs throughout the crop cycle (Figure 10). At the VE stage, TPE2 and TPE3 exhibited a higher frequency of high-precipitation conditions, whereas TPE1 showed a greater proportion of intermediate and low levels. Between VE–R2 and R3–R5, intermediate levels predominated across all TPEs, with greater homogeneity. In the R5–R8 stages, TPE1 showed a higher frequency of low-precipitation conditions, whereas TPE3 and TPE4 maintained a greater contribution of intermediate levels, indicating better water distribution.

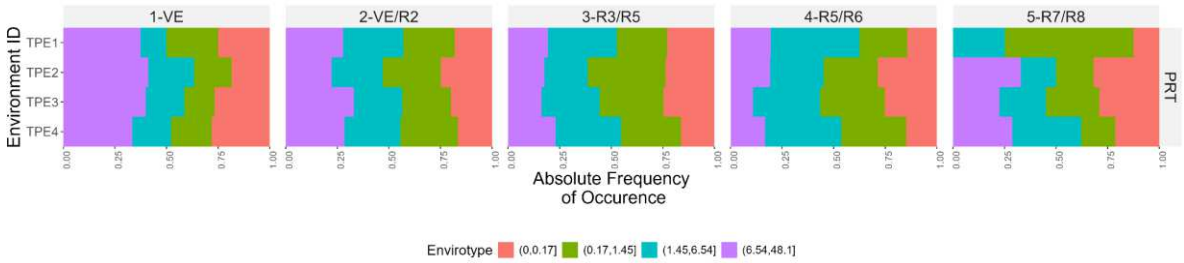


Fig. 10. Frequency distribution of precipitation (PRT, mm day^{-1}) across soybean phenological stages (VE, VE–R2, R3–R5, R5–R6 and R7–R8) in the four target populations of environments (TPEs).

Water availability is a key determinant of soybean yield, particularly during reproductive stages. The lower precipitation frequency observed in TPE1 during reproductive stages suggests greater susceptibility to transient water limitation during grain filling. In contrast, the more balanced precipitation distribution observed in TPE3 and TPE4 may favour maintenance of plant water status and reproductive development, contributing to greater

environmental stability. The precipitation deficit showed greater contrast among TPEs (Figure 11). At the VE stage, all TPE's exhibited a higher frequency of elevated deficit. Throughout VE–R2 and R3–R5, the deficit increased across TPEs, particularly in TPE1. In the final stages (R5–R8), TPE1 and TPE4 stood out with higher deficit levels, whereas TPE3 and TPE4 maintained lower and more stable values.

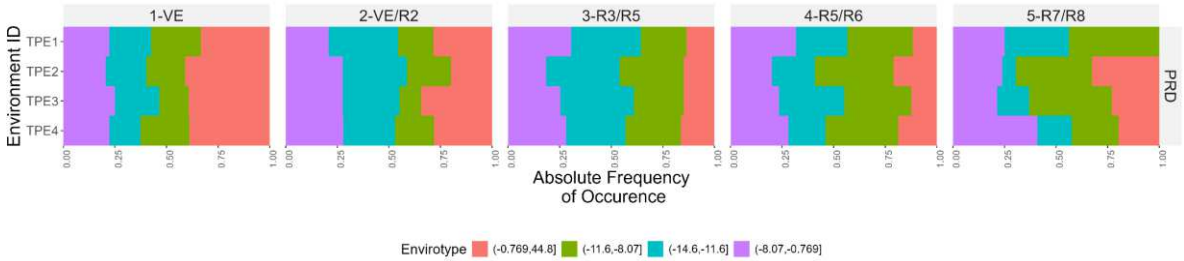


Fig. 11. Frequency distribution of precipitation deficit (PRD, mm day^{-1}) across soybean phenological stages (VE, VE–R2, R3–R5, R5–R6 and R7–R8) in the four target populations of environments (TPEs).

Precipitation deficit increases represent the imbalance between water supply and atmospheric demand and is a key indicator of drought stress in soybean production systems. Environments with elevated deficit, such as TPE1, are associated with increased drought stress. These findings are consistent with global evidence showing that water limitation is one of the primary factors reducing crop productivity under changing climatic conditions, as observed in TPE3 and TPE4, favor more stable crop performance [45]. Drought stress severely affects soybean physiology, leading to reductions in photosynthesis, nodulation, and nitrogen fixation, ultimately limiting yield [46].

The distribution of VPD showed consistent differences among TPEs (Figure 12). At the VE stage, TPE1 exhibited a higher frequency of elevated VPD values, whereas TPE3 and TPE4 showed more moderate conditions. Between VE–R2 and R3–R5, VPD increased across all TPEs, with greater intensity in TPE1. In the R5–R8 stages, the persistent atmospheric demand observed in TPE1 suggests conditions favouring physiological drought responses, potentially increasing stomatal limitation during reproductive development. Conversely, the more moderate VPD conditions observed in TPE3 and TPE4 may contribute to improved water-use efficiency and reproductive stability.

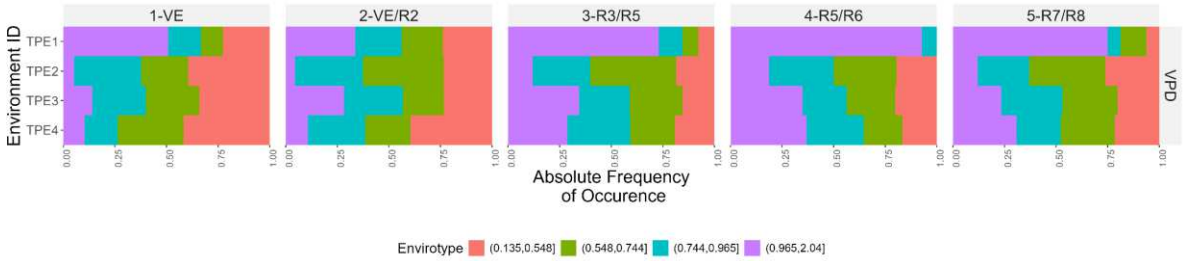


Fig. 12. Frequency distribution of vapor pressure deficit (VPD, kPa) across soybean phenological stages (VE, VE–R2, R3–R5, R5–R6 and R7–R8) in the four target populations of environments (TPEs).

Higher VPD increases atmospheric demand and drives transpiration, often leading to partial stomatal closure, reduced CO_2 assimilation, and lower photosynthetic efficiency under water-limited conditions. Even when soil moisture is adequate, elevated VPD can increase crop vulnerability to short-term drought events [47]. Consequently, environments with high VPD, such as TPE1, may experience greater physiological stress, whereas moderate VPD conditions, as observed in TPE3 and TPE4, tend to support improved water-use efficiency and yield stability.

The SDU showed consistent variation among TPEs. At the VE stage, all TPEs exhibited a higher frequency of elevated classes. During VE–R2 and R3–R5, intermediate classes predominated, with a slight tendency for higher sunshine duration in TPE1. In the R5–R8 stages, TPE1 maintained higher SDU values, whereas TPE2, TPE3 and TPE4 showed a more balanced distribution (Figure 13).

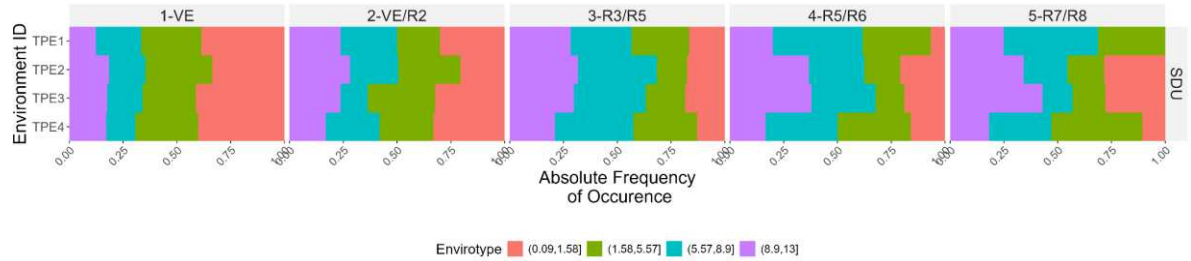


Fig. 13. Frequency distribution of actual sunshine duration (SDU, hours) across soybean phenological stages (VE, VE–R2, R3–R5, R5–R6 and R7–R8) in the four target populations of environments (TPEs).

Actual sunshine duration represents the effective availability of solar radiation for crop growth and is a key determinant of photosynthetic activity and biomass accumulation in soybean [48, 49]. Solar radiation interacts with temperature and atmospheric demand, influencing plant growth, evapotranspiration, and stress responses. However, the effect of sunshine duration is strongly modulated by its interaction with other climatic factors. Under conditions of high temperature and atmospheric demand, increased radiation may intensify evapotranspiration and plant water stress, limiting yield [45, 50]. The slightly greater sunshine duration observed in TPE1 during reproductive stages may increase radiation availability but may also intensify atmospheric demand when combined with elevated temperature and VPD. In contrast, the more balanced distribution observed in TPE2, TPE3 and TPE4 may favour more stable biomass accumulation across developmental stages [51, 52].

The envirotyping-based characterization of target population environments (TPEs) enabled the detection of predominant climatic patterns across soybean phenological stages during the 2023/24 growing season, providing a clearer understanding of the environmental drivers underlying genotype × environment interaction [8]. The integration of climatic covariates within the envirotyping framework enabled the identification of four physiologically distinct environmental groups, each contributing differently to genotype adaptation and yield expression. Overall, the identified envirotypes demonstrated that soybean adaptation results from the combined influence of thermal regime, atmospheric demand, and water availability throughout crop development. The temporal distribution of climatic drivers across

phenological stages likely imposes distinct physiological constraints affecting photosynthetic performance, plant water status, and reproductive development, ultimately shaping genotype adaptation patterns and the expression of genotype × environment interaction.

3.3 TPEs and grain yield performance

The association between target populations of environments (TPEs) and the grain yield performance of genotypes revealed consistent patterns that reinforce the role of envirotyping in interpreting genotype × environment (G×E) interaction and in defining breeding strategies. In general, a clear stratification of environments was observed in terms of mean productivity, experimental precision (CV), and heritability (H^2), indicating that the TPEs captured, in a biologically meaningful way, the environmental variability affecting the phenotypic expression of grain yield.

The analysis of genetic parameters by environment, considering exclusively the data presented in Table S3, highlights consistent differences among TPEs in terms of productivity, experimental precision (CV), and heritability (H^2), enabling a robust interpretation of the structure of G×E interaction.

Overall, TPE2 comprised environments with high productive performance, including Espumoso-E7 (5207.39 kg ha^{-1}), Condor-E3 (5075.76 kg ha^{-1}), and Palmeira das Missões-E11 (4991.35 kg ha^{-1}), all associated with low coefficients of variation (3.00–4.50%) and high heritability estimates (0.87–0.95). This pattern indicates high experimental quality and strong genetic control over trait expression, favouring selection efficiency. However, the inclusion of Giruá-E8 (3341.19 kg ha^{-1}; CV = 6.25%; H^2 = 0.80) within the same TPE demonstrates that, although a general pattern of high performance exists, relevant internal variability is present. Nevertheless, the predominance of environments with high productivity and high heritability suggests that TPE2 predominantly represents favourable conditions for the expression of genetic potential.

TPE4 exhibited the greatest productive amplitude among environments, ranging from 3853.30 kg ha^{-1} (Renascença-E13) to 5561.71 kg ha^{-1} (Irati-E10). This TPE includes highly productive environments, such as Pitanga-E12 (5333.99 kg ha^{-1}). The coefficients of variation in this group were higher (5.40–8.75%), indicating lower experimental precision in some environments, particularly Irati-E10 (CV = 8.75%). Heritability estimates, however, remained high (0.83–0.94), suggesting that despite greater phenotypic variability, the proportion of genetic variance is still substantial. These results characterise TPE4 as a group of heterogeneous environments, with strong variation in environmental conditions and, consequently, greater potential for G×E expression.

TPE1, represented by Cascavel-E2 (4783.96 kg ha^{-1}) and Cafelândia-E1 (4384.00 kg ha^{-1}), showed intermediate productivity, with moderate coefficients of variation (4.70–5.50%) and high heritability (0.81–0.91). This pattern indicates relatively stable environments, with good experimental quality and consistent levels of genetic control. The lower productive amplitude observed in this TPE suggests reduced environmental variability compared with the others, positioning it as representative of average growing conditions.

In contrast, TPE3 exhibited a more inconsistent pattern. Although it includes a high-yielding environment, Cruz Alta.1-E5 (5423.13 kg ha^{-1}), this was associated with relatively low heritability (H^2 = 0.40) and a high coefficient of variation (7.70%), indicating low

reliability in the genetic expression of the trait in this specific environment. The remaining environments within TPE3, Cruz Alta.2-E6 (4214.48 kg ha^{-1}; H^2 = 0.82) and Coxilha-E4 (3990.32 kg ha^{-1}; H^2 = 0.83), presented higher heritability estimates, but still with relatively high coefficients of variation (5.30–7.95%). This pattern suggests a stronger influence of environmental effects and a possible intensification of G×E interaction, reducing the predictability of selection response.

The comparison among TPEs indicates that environmental grouping was able to discriminate between environments not only based on mean productivity, but also on the quality of genetic estimates. TPE2 stands out due to the combination of high productivity, low CV, and high heritability, representing the most favourable group for selection. TPE4, despite presenting high heritability, exhibits greater productive and experimental heterogeneity, reflecting increased environmental variability. TPE1 shows an intermediate and more stable behaviour, whereas TPE3 reveals inconsistency, particularly due to the low heritability observed in one of its environments.

These findings reinforce that the use of TPEs enables a better understanding of G×E structure by demonstrating that environments with similar productivity levels may differ substantially in terms of experimental precision and genetic control of the trait. Consequently, breeding strategies should consider not only the productivity level of environments but also the quality of the genetic estimates associated with each TPEs.

4. Conclusion

TPE1 (Cafelândia-PR-E1; Cascavel-PR-E2) was characterized by moderate thermal and atmospheric conditions. TPE2 (Condor-RS-E3; Espumoso-RS-E7; Girua-RS-E8; Palmeira das Missões-RS-E11) showed greater climatic variability, particularly in temperature and atmospheric demand. TPE3 (Coxilha-RS-E4; Cruz Alta1-RS-E5; Cruz Alta2-RS-E6) presented the most stable environmental pattern associated with sunshine duration and similarly with photoperiod. TPE4 (Guarapuava-PR-E9; Irati-PR-E10; Pitanga-PR-E12; Renascença-PR-E13; Tibagi-PR-E14) represented the most restrictive environment, characterized by frequent precipitation deficit, and elevated vapor pressure deficit.

Regarding genotypic performance, genotypes G2-511IPRO, G9-NS5505 I2X, and G8-54IX57RSFI2X combined high yield and stability in TPE1, indicating broad adaptation to this environment. In contrast, G15-LI4E exhibited high yield potential but showed a stronger interaction with environmental conditions, suggesting specific adaptation rather than broad stability. In TPE2, genotypes G3-NS5115I2X, G11-LI0A, and G25-LI14O performed best, demonstrating superior productivity under warmer conditions with irregular water availability. In TPE3, characterized by greater climatic stability, genotypes G11-LI0A, G19-LI8I, and G22-LI11L exhibited superior performance, reflecting favorable responses in more predictable environments. In TPE4, the most restrictive environment, genotypes G5-51IX51RSFI2X, G11-LI0A, G8-54IX57RSFI2X, G17-LI6G, and G20-LI9J displayed greater stability and higher productivity, indicating their tolerance and adaptation under adverse conditions.

In conclusion, environmental stratification reinforces its strategic role in guiding plant breeding, as it reveals adaptation and stability patterns that support the selection of more efficient cultivars. In the context of accelerating climate change, future studies that improve

environmental characterization and develop methodologies capable of expediting the identification of more resilient and broadly adapted genotypes will be essential.

Declarations

Ethics approval and consent to participate Not applicable.

Consent for publication Not applicable.

Availability of data and materials The data that support the findings of this study are available from the corresponding author upon reasonable request.

Competing interests The authors declare that they have no competing interests.

Funding This work was supported by the Conselho Nacional de Desenvolvimento Científico e Tecnológico (CNPq), Brazil [Grant No. 132373/2024-6].

Authors Contributions

SMF: Conceptualization, Data curation, Formal analysis, Investigation, Methodology, Visualization, Writing –original draft. All authors read and approved the final manuscript. GB: Conceptualization, Supervision, Methodology, Writing – review & editing. CWA: Investigation, Writing – review & editing. SCT: contributed to the preliminary execution, interpretation and formal analysis. FAR: Writing – review & editing. TO: Methodology. LDF: Resources, Investigation. NFG: Resources. GVM: Supervision, Writing – review & editing. All authors read and approved the final manuscript.

Acknowledgements Not applicable.

Authors' information Not applicable.

5. References

1. CONAB. Crop Monitoring Report 2025/26– 9th Survey. Companhia Nacional de Abastecimento, Brasília, Brazil, 2025. https://www.conab.gov.br (accessed 20 January 2025).

2. Poudel S, Acharya B, Paudel B. Resilience of soybean cultivars to drought stress during flowering and early seed-setting stages. Sci Rep, 2023; 13:1277. doi: 10.1038/s41598-023-28354-0.

3. Araújo MS, Pereira GR, Chaves DFD, Costa-Neto G, Fritsche-Neto R. Optimizing soybean variety selection for the Pan-African Trial network using factor analytic models and envirotyping. Front Plant Sci, 2025; 16:1594736. doi 10.3389/fpls.2025.1594736.

4. Elmerich C, Nendel C, Stützel H. Identification of eco-climatic factors driving yields and genotype by environment interactions for yield in early maturity soybean using crop simulation. Agronomy, 2023; 13(2)322. doi:10.3390/agronomy13020322.
5. Doná S, Lemos LB, Carvalho EV, Moraes LLA. Evaluation, adaptability and agronomic performance of early cycle soybean cultivars in the municipalities of Brotas, Cândido Mota and Palmital in the state of São Paulo. Res Soc Dev, 2024; 13:e9413746362. doi:10.33448/rsd-v13i7.46362.
6. Mwiinga B, Sibiya J, Kondwakwenda A, Musvosvi C, Chigeza G. Genotype × environment interaction analysis of soybean (Glycine max (L.) Merrill) grain yield across production environments in Southern Africa. Field Crops Res, 2020; 256, 107922. doi:/10.1016/j.fcr.2020.107922.
7. Krause MD, Araújo MS, Costa-Neto G, Fritsche-Neto R. Using soybean historical field trial data to study genotype by environment variation and identify mega-environments with the integration of genetic and non-genetic factors. Agron J, 2025; 117:e70023. doi:10.1002/agj2.70023.
8. Costa-Neto G, Galli G, Fritsche-Neto R. EnvRtype: a software to interplay enviromics and quantitative genomics in agriculture. G3: Genes, Genomes, Genetics, 2021; 11, (4):1-20. doi:10.1093/g3journal/jkab040.
9. Yue H, Wang Y, Chen Z, Zhu J, Behera PP, Liu P, Yang H, Wei J, Bu J, Jiang X, Ma W. Assessing the role of genotype by environment interaction of winter wheat cultivars using envirotyping techniques in North China. Front Plant Sci, 2025; 16:1538661. doi:10.3389/fpls.2025.1538661.
10. Resende RT, Piepho HP, Rosa GJM, Silva FF, Resende MDV. Enviromics in breeding: applications and perspectives on envirotypic-assisted selection. Theor Appl Genet, 2021; 134:95–112. doi:10.1007/s00122-020-03684-z.
11. Sood R, Kumar V, Sharma A. AMMI and GGE biplot analysis for seed yield and stability performance of select buckwheat genotypes. Sci Rep, 2025; 15:36830. doi:10.1038/s41598-025-10939-6.
12. Corlouer E, Rincent R, Mangin B, Faure S, Le Gouis J, Allard V. Envirotyping within a multi-environment trial allowed identifying genetic determinants of winter oilseed rape yield stability. Theor Appl Gen, 2024; 137:164. doi:10.1007/s00122-024-04664-3.
13. Crespo-Herrera LA, Crossa J, Huerta-Espino J, Mondal S, Velu G, Juliana P, Vargas M, Pérez-Rodríguez P, Joshi AK, Braun HJ. Target Population of Environments for Wheat Breeding in India: Definition, Prediction and Genetic Gains. Front Plant Sci, 2021; 12:638520. doi:10.3389/fpls.2021.638520.
14. Gilbert C, Martin N. Using agro-ecological zones to improve the representation of a multi-environment trial of soybean varieties. Front Plant Sci, 2024; 15:1310461. doi:10.3389/fpls.2024.1310461.
15. Nasir B, Rahman SU, Ali A. Resilient soybean for a changing climate: analysis of traditional and emerging plant breeding technologies to address abiotic stresses. Acta Physiol Plant, 2025; 47:102. doi:10.1007/s11738-025-03847-9.
16. Pereira GR, Araújo MS, Chaves SFS, Nunes JAR, Carneiro PCS, Carneiro JES, Cruz CD. Exploring genotype-environment interactions in tropical soybean multi-environment trials. Euphytica, 2025; 221:124. doi:10.1007/s10681-025-03576-7.

17. Cooper M, Messina CD. Predicting the future of plant breeding: complementing empirical evaluation with genetic prediction. Crop Past Sci, 2014; 65(4):311–336. doi:10.1071/CP14007.
18. Olivoto T, Lúcio AD, da Silva JA, Marchioro VS, Souza VQ, Jost E. Mean performance and stability in multi-environment trials I: combining features of AMMI and BLUP techniques. Agron J, 2019; 111:2949–2960. doi:10.2134/agronj2019.03.0220.
19. Wickham H, Averick M, Bryan J, Chang W, McGowan LD, François R, Grolemund G, Hayes A, Henry L, Hester J, Kuhn M, Pedersen TL, Miller E, Bache SM, Müller K, Ooms J, Robinson D, Seidel DP, Spinu V, Takahashi K, Vaughan D, Wilke C, Woo K, Yutani H. Welcome to the tidyverse. J Open Source Softw, 2019; 4:1686. doi:10.21105/joss.01686.
20. R Core Team. R: a language and environment for statistical computing. Vienna: R Foundation for Statistical Computing, 2023. https://www.R-project.org/ (Accessed 25 April 2023).
21. Olivoto T, Lúcio ADC. metan: An R package for multi-environment trial analysis. Methods in Ecology and Evolution, 2020; 11:783–789. J Open Source Softw. doi:10.1111/2041-210X.13384.
22. Falconer DS, Mackay TFC. Introduction to quantitative genetics, 4th edn. Longman, Harlow, 1996.
23. Manjunath P, Shadakshari YG, Vijayakumar AG.Assessment of heritability and genetic advance in soybean. Journal of Oilseeds Res, 2020, 37(special issue). doi: 10.56739/jor.v37iSpecialissue.139463.
24. Nayak S, Mishra S, Sahoo B. Genetic variability, heritability and genetic advance in soybean. Int J Adv Biochem Res, 2024; 8:743–745. doi:10.33545/26174693.2024.v8.i11Sj.3015.
25. Argaw T. Multi-environment trials data analysis: linear mixed model-based approaches using spatial and factor analytic models. Front Res Met Anal. 2025; 10:1472282. doi: 10.3389/frma.2025.1472282.
26. Demelash H. Genotype by environment interaction, AMMI, GGE biplot, and mega environment analysis of elite *Sorghum bicolor* (L.) Moench genotypes in humid lowland areas of Ethiopia, Heliyon, 2024; 10, Issue 5, e26528. doi:10.1016/j.heliyon.2024.e26528.
27. Bocianowski J, Nowosad K, Szulc P. Genotype-environment interaction for grain yield in maize (*Zea mays* L.) using the additive main effects and multiplicative interaction (AMMI) model. J Appl Gen, 2024; 65(4):653-664. doi:10.1007/s13353-024-00899-4.
28. Costa-Neto GM, Volpato L, Fritsche-Neto R. Envirotyping for understanding and predicting genotype × environment interaction in plant breeding. Theor Appl Gen, 2024. doi:10.1007/s00122-024-04515-0.
29. Crossa J, Cornelius PL, Yan W. Biplots of linear-bilinear models for studying crossover genotype × environment interaction. Crop Sci, 2022; 42:619–633. doi:10.2135/cropsci2002.0619.
30. Pour-Aboughadareh A, Khalili M, Poczai P, Olivoto T. Stability Indices to Deciphering the Genotype-by-Environment Interaction (GEI) Effect: An Applicable Review for Use in Plant Breeding Programs. Plant, 2022; 2;11(3):414. doi:10.3390/plants11030414.

31. Piepho HP, Möhring J, Melchinger AE, Büchse A. BLUP for phenotypic selection in plant breeding. Euphytica, 2008; 161, 209–228. doi:10.1007/s10681-007-9449-8.
32. Smith AB, Cullis BR, Thompson R. The analysis of crop cultivar breeding and evaluation trials: an overview of current mixed model approaches. The J Agric Sci, 2015; 153:1–22. doi:10.1017/S0021859614000305.
33. Atroch AL, Nascimento IR, Farias FJC, Almeida LA, Sediyama T. Identificação de mega-ambientes e desempenho de genótipos de soja em múltiplos locais no Brasil. Pesq Agrop Brasil, 2020; 55:01754. doi:10.1590/S1678-3921.pab2020.v55.01754.
34. Sun W, Butler EE, Ainsworth EA. Projected long-term climate trends reveal the critical role of vapor pressure deficit for soybean production in the US Midwest. Sci The Total Env, 2023; 878:162960. doi:10.1016/j.scitotenv.2023.162960.
35. Zhang Z, Ober U, Erbe M, Zhang H, Gao N, He J, Li J, Simianer H. Improving the accuracy of whole genome prediction for complex traits using the results of genome-wide association studies. PLoS One, 2021; 16:0249714. doi:10.1371/journal.pone.0249714.
36. Burroughs CH, Montes CM, Moller CA, Mitchell NG, Michael AM, Peng B, Kimm H, Pederson TL, Lipka AE, Bernacchi CJ, Guan K, Ainsworth EA. Reductions in leaf area index, pod production, seed size, and harvest index drive yield loss to high temperatures in soybean. J Exp Bot, 2023; 74:1629–1641. doi:10.1093/jxb/erac503.
37. Djanaguiraman M, Prasad PVV, Boyle DL, Schapaugh WT. High temperature stress and soybean: physiological responses and underlying mechanisms. Crop Sci, 2019; 59(6), 2554–2566. doi:10.2135/cropsci2019.04.0242.
38. Liu Y, Mizuta K, Morokuma M, Toyota M. Combined Drought and Heat Stress Reduce Soybean Yield by Limiting the Number of Nodes Per Branch in a Temperature Gradient Chamber. Journal of Agronomy and Crop Sci, 2025; 211:6, e70138. doi:10.1111/jac.70138.
39. Battisti R, Sentelhas PC, Pilau FG. New agroclimatic approach for soybean sowing dates recommendation: a case study. Rev Brasil Engen Agrí Amb, 2014; 18:1149–1156 doi:10.1590/1807-1929/agriambi.v18n11p1149-1156.
40. Ding C, Alghabari F, Rauf M, Zhao T, Javed MM, Alshamrani R, Ghazy AH, Al-Doss AA, Khalid T, Yang SH, Shah ZH. Optimization of soybean physiochemical, agronomic, and genetic responses under varying regimes of day and night temperatures. Front Plant Sci, 2024; 14:1332414. doi:10.3389/fpls.2023.1332414.
41. Du Y, Zhao Q, Chen L, Yao X, Xie F. Effect of Drought Stress at Reproductive Stages on Growth and Nitrogen Metabolism in Soybean. Agron, 2020; 10(2):302. doi:10.3390/agronomy10020302.
42. Port ED, Carvalho IR, Colet CF, Loro MV, Pradebon LC, Sangiovo JP, Silva JAG, Bandeira WJA. Relationships between meteorological variables and the productive performance of soybean lines. Pesq Agro Brasil, 2025; 60:e03939. doi:10.1590/S1678-3921.pab2025.v60.03939.
43. Wang C, Sun A, Zhu LJ, Liu M, Zhang Q, Wang L, Gao X. Drought and rewatering effects on soybean photosynthesis, physiology and yield. PeerJ, 2025; 13:19658. doi:10.7717/peerj.19658.

44. Grassini P, Torrion JA, Yang H, Rees J, Andersen D, Cassman KG, Specht JE. Soybean yield gap analysis in the western U.S. Corn Belt. Field Crops Res, 2015; 179:86–96 doi:10.1016/j.fcr.2015.04.017.
45. Zipper SC, Qiu J, Kucharik CJ. Drought effects on U.S. maize and soybean production: spatiotemporal patterns and historical changes. Enviro Res Lett, 2020; 15:094021. doi:10.1088/1748-9326/ab7c3b.
46. Lobell DB, Schlenker W, Costa-Roberts J. Climate trends and global crop production since 1980. Science, 2011; 333(6042), 616–620. doi:10.1126/science.1204531.
47. Kunert KJ, Vorster BJ, Fenta BA, Kibido T, Dionisio G, Foyer CH. Drought stress responses in soybean. Front Plant Sci, 2016; 7:159. doi:10.3389/fpls.2016.00159.
48. Messina CD, Hammer GL, McLean G, Cooper M, Oosterom EJV. Limited-transpiration trait may increase maize drought tolerance in the US Corn Belt. Field Crops Res, 2022; 279:108457. doi:10.1016/j.fcr.2022.108457.
49. Monteith JL. Climate and the efficiency of crop production in Britain. Phil Trans Royal Soc B, 1977; 281:277–294. doi:10.1098/rstb.1977.0140.
50. Sinclair TR, Muchow RC. Radiation use efficiency. Adv Agron, 1999; 65:215–265. doi:10.1016/S0065-2113(08)60914-1.
51. Hatfield JL, Prueger JH. Temperature extremes: Effect on plant growth and development. Weather Clim Extrem, 2015; 10:4-10. doi:10.1016/j.wace.2015.08.001.
52. Board JE, Kahlon CS. Soybean yield formation: What controls it and how it can be improved. Agronomy Journal, 2011; 103:968–977. doi:10.2134/agronj2011.0007.
53. Purcell LC, Ball RA, Reaper JD, Vories ED. Radiation use efficiency and biomass production in soybean at different plant population densities. Crop Sci, 2002; 42:172–177. doi:10.2135/cropsci2002.1720.

Supplementary Files

This is a list of supplementary files associated with this preprint. Click to download.

- SupplementaryMaterial.docx